



# CHORUS

This is the accepted manuscript made available via CHORUS. The article has been published as:

## Topological Surface States in Dense Solid Hydrogen

Ivan I. Naumov and Russell J. Hemley

Phys. Rev. Lett. **117**, 206403 — Published 10 November 2016

DOI: [10.1103/PhysRevLett.117.206403](https://doi.org/10.1103/PhysRevLett.117.206403)

# Topological surface states in dense solid hydrogen

Ivan I. Naumov<sup>1</sup> and Russell J. Hemley<sup>2,3</sup>

<sup>1</sup>*Geophysical Laboratory, Carnegie Institution of Washington, Washington DC 20015, USA*

<sup>2</sup>*Department of Civil and Environmental Engineering, George Washington University,  
Washington, DC 20052, USA*

<sup>3</sup>*Lawrence Livermore National Laboratory, Livermore CA 94550, USA*

Metallization of dense hydrogen and associated possible high-temperature superconductivity represents one of the key problems of physics. Recent theoretical studies indicate that before becoming a good metal compressed solid hydrogen passes through semimetallic stage. We show that such semimetallic phases predicted to be the most stable at multimegabar (~300 GPa) pressures are not conventional semimetals: they exhibit topological metallic surface states inside the bulk “direct” gap in the two-dimensional surface Brillouin zone, that is, metallic surfaces may appear even when the bulk of the material remains insulating. Examples include hydrogen in the *Cmca-12* and *Cmca-4* structures, the behavior of which can be contrasted with *Pbcn* hydrogen, which also has metallic surface states but of non-topological nature. The results provide predictions for future measurements, including probes of possible surface superconductivity in dense hydrogen.

The behavior of hydrogen at high pressure is currently a subject of intense interest. At multimegabar pressures, the material is predicted to exhibit high- $T_c$  superconductivity, superfluidity, and other unique metallic properties in its high-density solid and fluid phases [1-4]. Recent experimental and theoretical investigations suggest that at pressures beginning above 250 GPa solid hydrogen can transform into molecular  $Cmca-12$  [5-11] and/or  $Cmca-4$  [9-15] phases; the former can be insulating or semimetallic, whereas the latter is only semimetallic. We show that these phases are not conventional semimetals in that they have pronounced Shockley metallic surface states (SSs) of topological nature. These states are controlled by Zak's phase and form inside the "direct gap" between conduction and valence bands. They cover the whole two-dimensional surface Brillouin zone (BZ) in the case of  $Cmca-12$  and only part of the zone for  $Cmca-4$ . Moreover, in  $Cmca-12$  the SSs can coexist with the insulating bulk, whereas in  $Cmca-4$  both surface and bulk states are always metallic. These results have important implications for characterizing semimetallic, metallic, and superconducting states of hydrogen being explored experimentally at multimegabar pressures.

In his seminal 1939 paper Shockley showed how SSs appear in one-dimensional (1D) centrosymmetric crystal as the lattice parameter  $a$  decreases [16]. At some critical point  $a_c$ , the valence and conduction and valence bands cross, leaving two surface states within the bulk energy gap; at the  $a_c$  the latter closes and then immediately opens up becoming "inverted". Much later, Zak realized that Shockley-type SSs have in fact a topological character [17]. He demonstrated that when the surface coincides with the symmetry centers, the existence or absence of the corresponding SSs is decided by the topology of the band below the gap. Of special interest in the general theory of SSs is the case when the surface is taken between the atoms at the potential maxima, which is the situation that Shockley discussed in his pioneering work. In this case, speaking in more contemporary terms, the existence of SSs is related to the sum of all Zak's phases  $Z$  below the gap [18,19]. The SSs exist when the total phase is  $\pi$  and does not exist when it is 0. From the topological point of view, Shockley's critical parameter  $a_c$  is nothing but the point of topological transition at which the Zak's phase discontinuously changes from 0 to  $\pi$ .

Though Shockley and Zak considered only a simple 1D model, their results can be extended to systems of higher dimensions. As established recently, criteria for the existence of

SSs are still applicable in centrosymmetric zero-gap semiconductors where the conduction and valence bands touch each other at points (2D *massless graphene-like* systems [20-22]) or along lines (3D *line-node topological semimetals* [23,24]). In such 2D and 3D materials, the existence of SSs with a particular momentum  $\mathbf{k}_{\parallel}$  is controlled by the value of Zak's phase  $Z(\mathbf{k}_{\parallel})$  obtained by the integration across the BZ perpendicular to the edge/surface [20-24]. As in the 1D case, the SSs exist if  $Z(\mathbf{k}_{\parallel})$  is  $\pi$  (inverted band gaps) and do not if it is 0. For this, however, the phase  $Z$  becomes dependent on a new parameter  $\mathbf{k}_{\parallel}$ , which can be critical similar to the lattice parameter  $a$  in the 1D case. The possible values of  $Z(\mathbf{k}_{\parallel})$ , 0 or  $\pi$ , are completely defined by the positions of the band-contact points or lines. Thus, in graphene with zigzag edges, the SSs states exist within a finite  $\mathbf{k}_{\parallel}$ -interval corresponding to the projection of the Dirac points  $\mathbf{K}$  and  $\mathbf{K}'$  on the  $\mathbf{k}_{\parallel}$  axis; within this interval  $Z(\mathbf{k}_{\parallel}) = \pi$  [20-22].

The line-node topological semimetals (LNTSs) can be viewed as 3D analogs of graphene. Instead of two separated Dirac points, they have an infinite number of effective Dirac points merged together – band-contact lines lying at the Fermi level exactly (nodal lines) [23-25]. In LNTSs, the SSs appear within the whole  $\mathbf{k}_{\parallel}$ -area where  $Z(\mathbf{k}_{\parallel}) = \pi$ ; this area is limited by the projection of the nodal line (loop) onto the surface plane of interest [23-25]. The SSs are completely dispersionless and therefore characterized by an infinite density of states (DOS) at the Fermi level  $E_F$  [23-25]. This unphysical DOS reflects the fact that the LNTSs are actually idealized models where the band-contact line lies at the  $E_F$  [23]. In real materials, the probability that band-contact lines coincide with the  $E_F$  is vanishingly small [23]. Many systems, however, can be considered as “approximate” LNTSs where the contact lines have some dispersion and so do the SSs. Though SSs in “approximate” LNTSs acquire some dispersion, they still retain their topological nature and their existence can be predicted by the bulk Zak's phase [25,26]. Remarkably, the bulk Zak's phase is capable of capturing not only the difference between the surfaces of distinct orientations, but also the difference between the distinct terminations (if any) for a given orientation [21,22,24]. Such a nontrivial correspondence between the Zak's phases and surface terminations appears owing to the convention that the surface is made by cutting a solid *between the primitive unit cells* [20-22] (we will refer to this as a *cutting rule*). This rule says that once the surface orientation and termination are specified they automatically specify the bulk primitive unit cell.

As a result of varying parameters in the crystal potential, the band crossing line (loop) can gradually disappear by shrinking to some point or “sinking” in the BZ boundary; this corresponds to a semimetallic-to-insulator transition. In the insulating state, the phase  $Z(\mathbf{k}_{\parallel})$  will become either 0 or  $\pi$  for all  $\mathbf{k}_{\parallel}$  in the surface BZ [21,22]. The result depends on which part of the step-like distribution  $Z(\mathbf{k}_{\parallel})$  is extending. If  $Z(\mathbf{k}_{\parallel})$  is  $\pi$  everywhere, then the system should behave as a topological insulator: they are insulating in the bulk but necessarily have metallic surface states [21,22]. This is the case of *Cmca*-12 as we show below.

We begin with the *Cmca*-4 structure, which geometrically is close to hexagonal graphite: its primitive unit cell consists of four atoms and its layers are arranged in an ABAB sequence (Fig. 1). The calculated band structure of *Cmca*-4 hydrogen at 300 GPa shows that this system is in fact an “approximate” LNTS (Fig. 1d). The valence and conduction bands intersect each other in a linear (Dirac-like) fashion for all the segments starting from the Y-point. Since the Dirac-like points must lie on band contact lines normal to the corresponding segments [27], one can expect that they all belong to *one* band-crossing loop lying in the *xy* plane and encircling the point Y. Such a loop should induce SSs localized on a (001) surface. There are two possible terminations associated with this surface orientation. The first one breaks the long (weak) interlayer chemical bonds, whereas the second breaks the short (strong) intralayer bonds. According to the cutting rule, these two terminations correspond to two different primitive unit cells shown in Fig. 2 (yellow rectangles in *a* and *b*). Hereafter, we call these terminations/unit cells “type *a*” and “type *b*”. Since we treat the surfaces as boundary planes of the films repeated periodically in space at equal vacuum gaps, such films should be built from the complete bulk primitive unit cells as building blocks. Their thickness therefore can be specified by the number of bulk primitive cells stacked along the *z* axis (*n*). It is easy to see that an *n*-unit-cell thick film organized from type *a* unit cells contains *n* molecular layers A and *n* molecular layers B (see Figs. 1 and 2). At the same time an *n*-unit-cell thick film organized from the type *b* unit cells contains *n*-1 molecular layers A, *n* molecular layers B (both inside the film), and additionally two atomic surface layers.

To check that the band-crossing loop and the corresponding SSs exist, we calculated the phases  $Z(\mathbf{k}_{\parallel})$  across the BZ in the *z* direction for both choices of the unit cell (Figs. 2c,d). We treated our system as if it were an ideal LNTSs; *i.e.* we assigned the number of “occupied” bands

at each  $\mathbf{k}_{\parallel}$  to be 2 (see the Supplemental Material [28]). For both cases the Zak's phase is quantized; *i.e.* it takes only values 0 and  $\pi$ . For the type *a* case, the Zak's phase is 0 almost everywhere in the surface BZ except relatively small areas around the  $\bar{Y}$  points (panel *c*). In going from type *a* to *b*, all the  $Z(\mathbf{k}_{\parallel})$  values shift by  $\pi$ , so that all the 0 phases become  $\pi$  and vice versa. These results suggest that in the type *a* case the SSs will cover a relatively small ellipse-like area around the  $\bar{Y}$  point, with the major radii almost reaching the  $\bar{U}$  points, whereas in the type *b* case – a significant part of the surface BZ centered at  $\bar{\Gamma}$ .

Direct calculations of surface electronic structure for 4-unit-cell thick films of H show that this is indeed the case (Fig. 3); the calculations for thicker films lead only to slightly different quantitative results. The surface bands obtained can be identified indicated by of thick black curves that cross the  $E_F$ . For type *a*, they appear around the  $\bar{Y}$  point, in agreement with Fig. 2*c*. In contrast, for type *b* they are realized everywhere in the surface BZ, but not in the vicinity of the  $\bar{Y}$  point, again in accordance with the Zak's phase calculations. We thus see that the stronger the broken bonds, the larger is the  $\mathbf{k}$ -area covered by the corresponding SSs; this allows one to interpret the SSs as dangling bond surface states. Notably, upon moving away from their “natural habitats”, the SSs gradually *turn* into bulk states, as shown by the thick red curves in Fig. 3. This reflects their topological nature and intimate relationship to the bulk electronic structure.

Figure 3 shows the SSs always appear in pairs, almost in the middle of the corresponding band gaps. One surface band falls out of the allowed bulk *valence* band and the other from the allowed *conduction* bulk band. Due to the presence of inversion symmetry, they are either symmetric or anti-symmetric with respect to the operation  $\mathbf{r} \rightarrow -\mathbf{r}$ . They do not coincide in energy because the opposite sides of the film still “feel” each other. However, they become exactly degenerate as the film becomes infinitely thick. It is straightforward to prove using Shockley's arguments [16] that the SSs must be *metallic*. Indeed, in a *Cmca-4* (001) hydrogen film there is *one more* band in the lowest, valence part of the spectrum relative to the similar effective bulk system. Therefore, this additional (surface) band must be partially occupied with electrons.

The charge distributions of the lower SS at different high-symmetry points in the  $x=0$  plane are given in Fig. 4. One can see that in the case of the type *a* termination, the density is

mainly localized in the first and third surface layers, whereas for type *b* termination in the two upper atomic layers (Fig. 4a,b). Further, it is easy to see that the charge on the opposite surfaces is located on the *different non-overlapping sublattices*. All sublattices corresponding to one surface can be obtained from the sublattices corresponding to the opposite surface by the inversion symmetry ( $\mathbf{r} \rightarrow -\mathbf{r}$ ). The metallization of the surface for type *b* termination seems natural: in this case the molecular (strong) bonds on the surface are broken. The situation, however, is not as trivial for case *a* termination, which preserves the “H<sub>2</sub>” molecular structure of the surface layer. Even in this case the electronic structure of the layer is *metallic* in character and the wave function is localized essentially on only one of the two H atoms (Fig. 4a).

We now proceed to the orthorhombic *Cmca*-12 phase, which shares with *Cmca*-4 the same space group but has a different number of atoms per primitive unit cell (12; Fig. 5a). At 300 GPa, this phase is a semimetal where the indirect band gap is closed due to lowering of the conduction band at the Y point below the  $E_F$  (Fig. 5b). In order to check the existence of SSs on the surfaces normal to the *x*, *y*, and *z*, we calculated Zak’s phases along the shortest reciprocal lattice vectors  $\mathbf{G}_1$ ,  $\mathbf{G}_2$ , and  $\mathbf{G}_3$  using conventional (non-primitive) unit cell with 24 atoms. We treated the system as if it was a real dielectric by assigning the number of occupied bands to be 12 at each  $\mathbf{k}_{\parallel}$ . The phases were measured relative to their ionic [29] counterparts. We found them to be zero for all  $\mathbf{k}_{\parallel}$  if they are integrated along the  $\mathbf{G}_1$  (*x*) and  $\mathbf{G}_2$  (*y*) directions. However, they are all  $\pi$  if integrated along the  $\mathbf{G}_3$  (*z*) direction. This means that the localized SSs should form on both (001) surfaces of a *Cmca*-12 slab provided that the latter is organized from the complete bulk unit cells [30]. The direct calculations of the band structure confirm that this is indeed the case (Fig. 5c). As for *Cmca*-4, we can see that there are two surface states that cross the  $E_F$ . Now, however, they cover the whole surface BZ. Due to the presence of the center of symmetry, these states are either symmetric or antisymmetric with respect to the inversion center ( $\mathbf{r} \rightarrow -\mathbf{r}$ ), as illustrated in Fig. 5d for the  $\bar{S}$  point. Correspondingly, they become degenerate if the film is thick enough. It is important that the SSs appear even *before* the system becomes semimetallic in the bulk.

Experimentally, distinguishing between possible surface and bulk conductivities can be challenging, as is the case for topological insulators [28]. When the bulk is still insulating but the surface becomes metallic, the optical conductivity at frequencies of order  $<0.2$  eV will be

completely determined by surface states lying within the bulk energy gap [28]. In the *Cmca-4* phase, bulk and surface conductivities always coexist, as mentioned above. For this structure, disentangling the surface and bulk contributions can be facilitated by specific behavior of the latter. It turns out that low-frequency bulk conductivity of *Cmca-4* hydrogen parallels that of graphite because the two materials resemble each other both structurally and electronically [31-33]. Using the Kubo-Greenwood formula we found that like graphite, the zero-temperature conductivity per layer,  $\sigma^{2D}$ , of *Cmca-4* hydrogen is very close to the universal value of  $\pi e^2/2h$  predicted for monolayer graphene [34,35] (in our case  $\sigma^{2D} \sim 1.07 \times \pi e^2/2h$ ). Moreover, the bulk optical conductivity remains to be close to this universal value at finite temperatures in the range of photon energies between 0.2 and 1.0 eV, as in graphite. This implies that any noticeable change in the total conductivity within this range should be solely due to the surface contribution. We expect that this contribution is higher in amplitude due to elevated DOS at the  $E_F$  in the surface layer. The local DOS at the  $E_F$  significantly increases upon formation of the (001) surfaces—by a factor of 3 and 10 for type *a* and *b* terminations, respectively (Fig. S3). The local DOS for the atoms belonging to the central layer is typical for bulk *Cmca-4* hydrogen, where the  $E_F$  is in the minimum of DOS. The increase in this quantity as one approaches the surface of the type *b*, for example, is explained by the surface states around the  $\bar{Y}$  point (Fig. 3b).

Different high-pressure structures of hydrogen are prone to have metallic SSs, but the existence of such SSs cannot always be predicted from the corresponding bulk band structures. For example, the *Pbcn* structure that has been used to interpret experimental data for the phase IV [36-37] exhibits pronounced “non-topological” SSs despite the absence of the bulk-surface correspondence discussed above [28]. We believe that similar effects should take place even in fluid molecular hydrogen undergoing pressure-induced metallization process via pseudogap closure. In this case, dangling bonds related to those identified here at the surface lead to the additional localized states in the pseudogap [38] thereby increasing the DOS at  $E_F$ . The system can reach a point at which states at  $E_F$  are no longer localized, and these critical metallic states are likely to be confined to the surface rather than to be bulk. Topological SSs similar to those discussed here for hydrogen can also form in some simple *sp* metals. For example, the pronounced Shockley states found earlier in Be on its (0001) surface around the  $\bar{\Gamma}$  point [39] could have been also predicted from Zak’s phase calculations. Due to their topological nature, these states are relatively flat; according to Ref. [40] the local DOS at the  $E_F$  is four times larger

than in the bulk. It has been suggested that such a situation can trigger an unusual form of surface superconductivity with very high  $T_c$  [40]. By analogy, one can expect the existence of such surface superconductivity in compressed hydrogen.

This research was supported by EFree, an Energy Frontier Research Center funded by the U.S. DOE, Office of Science, Basic Energy Sciences (award DE-SC0001057). The infrastructure and facilities used were supported by the U.S. DOE/NNSA (award DE-NA-002006, CDAC). Work at LLNL was performed under the auspices of the DOE (contract DE-AC52-07NA27344).

## References

1. V. L. Ginzburg, *Physics- Uspekhi* **42**, 353 (1999).
2. N. W. Ashcroft, *Phys. Rev. Lett.* **21**, 1748 (1968).
3. H. K. Mao and R. J. Hemley, *Rev. Mod. Phys.* **66**, 671 (1994).
4. J. M. McMahon, M. A. Morales, C. Pierleoni and D. M. Ceperley, *Rev. Mod. Phys.* **84**, 1607 (2012).
5. M. I. Eremets and I. A. Troyan, *Nature Mater.* **10**, 927 (2011).
6. R. P. Dias, O. Noked, and I. F. Silvera, arXiv:1603.02162v2.
7. C. J. Pickard and R. J. Needs, *Nat. Phys.* **3**, 473 (2007).
8. S. Lebègue, C. M. Araujo, D. Y. Kim, M. Ramzan, H. K. Mao, and R. Ahuja. *PNAS*, **109**, 9766 (2012)
9. C. J. Pickard, M. Martinez-Canales, and R. J. Needs, *Phys. Rev. B* **85**, 214114 (2012); **86**, 059902(E) (2012).
10. S. Azadi, W. M. C. Foulkes, and T. D. Kühne, *New Journal of Physics* **15**, 113005 (2013).
11. Azadi, B. Monserrat, W. M. C. Foulkes and R. J. Needs, *Phys. Rev. Lett.* **112**, 165501 (2014).
12. A. F. Goncharov, J. S. Tse, H. Wang, J. Yang, V. V. Struzhkin, R. T. Howie, and E. Gregoryanz, *Phys. Rev. B* **87**, 024101 (2013).
13. K. A. Johnson and N. W. Ashcroft, *Nature* **403**, 632 (2000).
14. J. M. McMahon and D. M. Ceperley, *Phys. Rev. Lett.* **106**, 165302 (2011).
15. H. Liu, L. Zhu, W. Cui, and Y. Ma, *J. Chem. Phys.* **137**, 074501(2012).
16. W. Shockley, *Phys. Rev.* **56**, 317 (1939).
17. J. Zak, *Phys. Rev. B* **32**, 2218 (1985).

18. M. Xiao, Z. Q. Zhang and C. T. Chan, Phys. Rev. X **4**, 021017 (2014).
19. M. Xiao, G. Ma, Z. Yang, P. Sheng, Z. Q. Zhang and C. T. Chan, Nature Phys. **11**, 240 (2015).
20. S. Ryu and Y. Hatsugai, Phys. Rev. Lett. **89**, 077002 (2002)
21. P. Delplace, D. Ullmo and G. Montambaux, Phys. Rev. B **84**, 195452 (2011).
22. T. Kariyado and Y. Hatsugai, Phys. Rev. B **90**, 085132 (2014).
23. A. A. Burkov, M. D. Hook, and L. Balents, Phys. Rev. B **84**, 235126 (2011).
24. R. Takahashi and S. Murakami, Phys. Rev. B **88**, 235303 (2013).
25. T. T. Heikkilä, N. B. Kopnin and G.E. Volovik, Pis'ma v ZhETF **94**, 252 (2011).
26. R. Xiao, F. Tasnádi, K. Koepnik, J. W. F. Venderbos, M. Richter, and M. Taut, Phys. Rev. B **84**, 165404 (2011).
27. C. Herring, Phys. Rev. **52**, 365 (1937).
28. See Supplemental Material at <http://link.aps.org/supplemental/.....>, which contains Refs [41-46] details of calculations and more discussion.
29. R. D. King-Smith and D. Vanderbilt, Phys. Rev. B **47**, 1651(1993).
30. The "topological" character of the *Cmca*-12 phase can be easily checked. By increasing the lattice parameter along the *z* axis and keeping all the other structural parameters the same, one can induce a band contact line in the *xy* plane around the Y point, similar to that in *Cmca*-4.
31. I. I. Naumov, R. E. Cohen, and R. J. Hemley, Phys. Rev. B **88**, 045125 (2013).
32. R. E. Cohen, I. I. Naumov, and R. J. Hemley, PNAS, **110**, 13757 (2013).
33. I. I. Naumov and R. J. Hemley, Acc. Chem. Res. **47**, 3551 (2014).

34. A. B. Kuzmenko, E. van Heumen, F. Carbone, and D. van der Marel, Phys. Rev. Lett. **100**, 117401 (2008).
35. K. F. Mak, L. Ju, F. Wang, T.F. Heinz, Solid State Comm., **152**, 1341 (2012).
36. R. T. Howie, C. L. Guillaume, T. Scheler, A. F. Goncharov, and E. Gregoryanz, Phys. Rev. Lett. **108**, 125501 (2012).
37. C. S. Zha, Z. Liu, and R. J. Hemley, Phys. Rev. Lett. **108**, 146402 (2012)
38. N. F. Mott, *Metal-Insulator Transitions*, Taylor & Francis (London, New-York, Philadelphia, 1990) 286 pp.
39. E. V. Chulkov, V. M. Silkin, and E. N. Shirykalov, Surf. Sci., **188**, 287 (1987).
40. T. Balasubramanian, E. Jensen, X. L. Wu and S. L. Hulbert, Phys. Rev. **B** 57, R6866 (1998).
41. X. Gonze, B. Amadon, P.M. Anglade, J.-M. Beuken, F. Bottin, P. Boulanger, F. Bruneval, D. Caliste, R. Caracas, M. Cote, T. Deutsch, L. Genovese, Ph. Ghosez, M. Giantomassi, S. Goedecker, D. Hamann, P. Hermet, F. Jollet, G. Jomard, S. Leroux, M. Mancini, S. Mazevet, M. J. T. Oliveira, G. Onida, Y. Pouillon, T. Rangel, G.-M. Rignanese, D. Sangalli, R. Shaltaf, M. Torrent, M. J. Verstraete, G. Zérah, J.W. Zwanziger, Computer Physics Commun, **180**, 2582 (2009).
42. H. J. Monkhorst and J. D. Pack, Phys. Rev. B, **13**, 5188 (1976).
43. R. Resta and D. Vanderbilt, *Physics of Ferroelectrics: A Modern Perspective (Topics in Applied Physics vol. 105)*, eds., C. H. Ahn, K. M. Rabe and J.-M. Triscone (Springer, Berlin, 2007) pp. 31-68.
44. C. Durand, X.-G. Zhang, S. M. Hus, C. Ma, M. A. McGuire, Y. Xu, H. Cao, I. Miotkowski, Y. P. Chen, and A-P. Li, Nano Lett., **16** , 2213 (2016).
45. K. Hofer, C. Becker, D. Rata, J. Swanson, P. Thalmeier, and L. H. Tjeng, PNAS, **111**, 14979 (2014).
46. L. L. Li, W. Xu, and F. M. Peeters, J. Appl. Phys., **117**, 175305 (2015).

## Figures

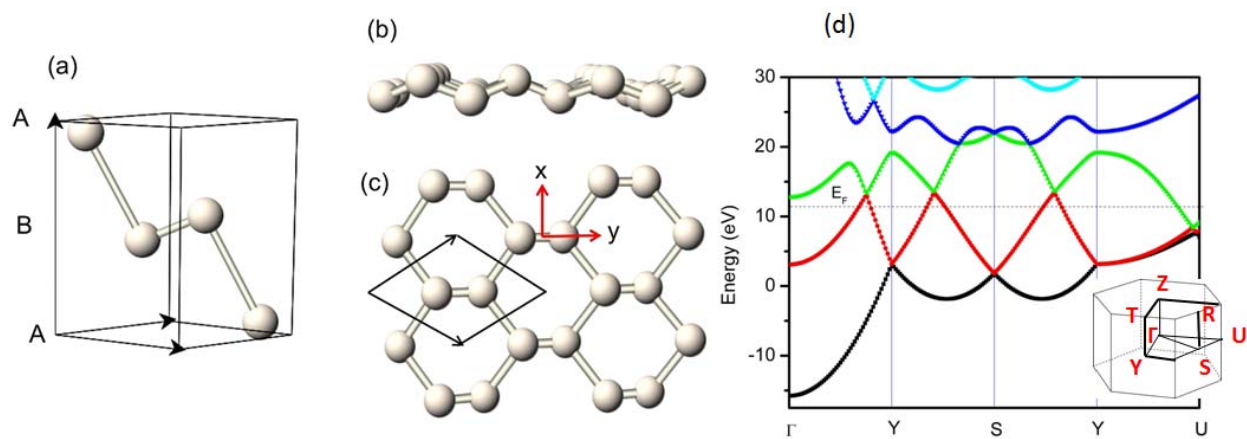


**Figure 1.** Crystal and band structures of the hydrogen  $Cmca-4$  phase. (a) primitive unit cell, (b) side and (c) top of a single layer. (d) Segments that involve the Y- point. The conduction and valence band intersections only approximately coincide with the Fermi level, indicating that the Fermi surface consists of small electron and hole pockets.

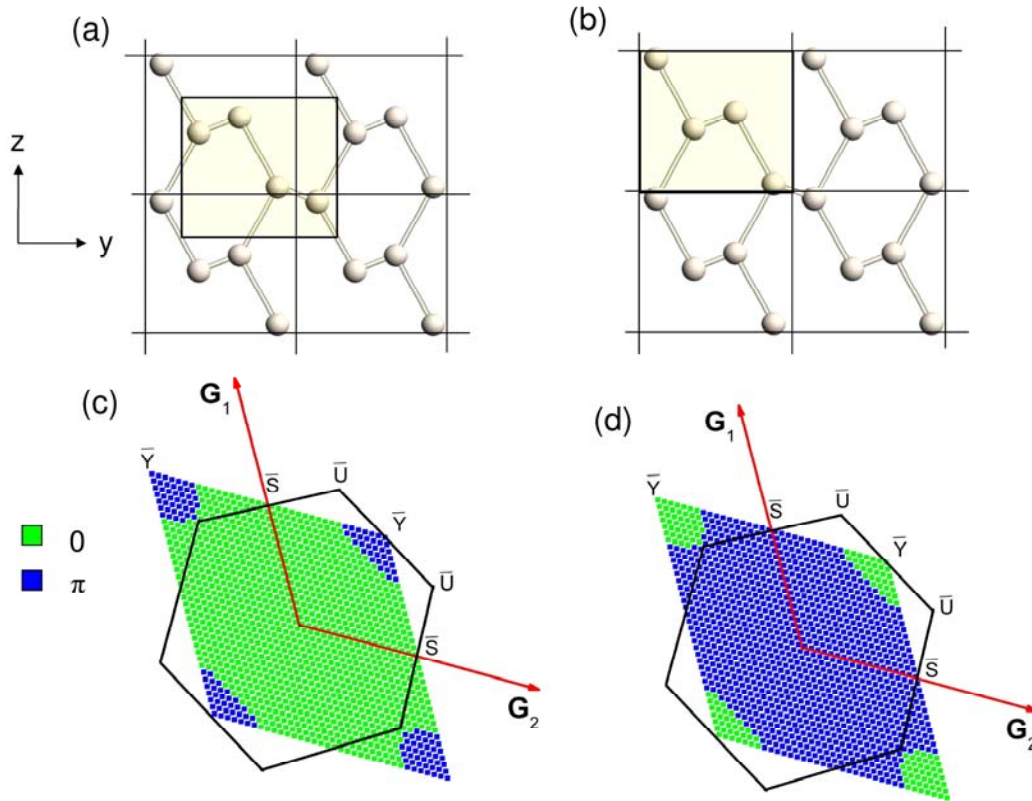


**Figure 2.** (a,b) Two choices of the primitive unit cell corresponding to two different surface terminations parallel to the  $xy$  plane, shown by yellow rectangles. For simplicity, we show the unit cells projected on the plane that contains all the 4 atoms shown in Fig. 1a. (c and d) Zak's phase  $Z$  as a function of  $\mathbf{k}_{\parallel}$  for the unit cells (a) and (b), respectively. The  $\mathbf{k}_{\parallel}$ -points are given on a  $36 \times 36$  grid associated with the two in-plane reciprocal vectors,  $\mathbf{G}_1$  and  $\mathbf{G}_2$ . The  $\mathbf{k}$ -point labels correspond to those presented in Fig. 1d. The phases  $0, \pi$  are shown in green and blue, respectively.

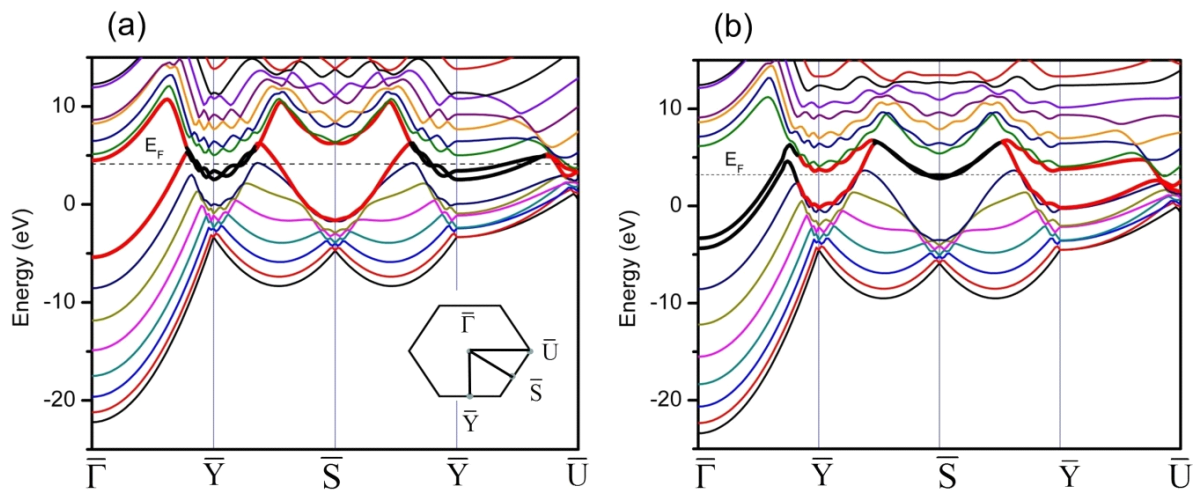


**Figure 3.** Two-dimensional energy bands of hydrogen in a 4-unit-cell thick  $Cmca-4$  structure. (a) Terminations that break long (weak) bonds on both sides of the film and (b) terminations that break short (strong) bonds. The surface bands are indicated by thick black curves that cross the  $E_F$ .

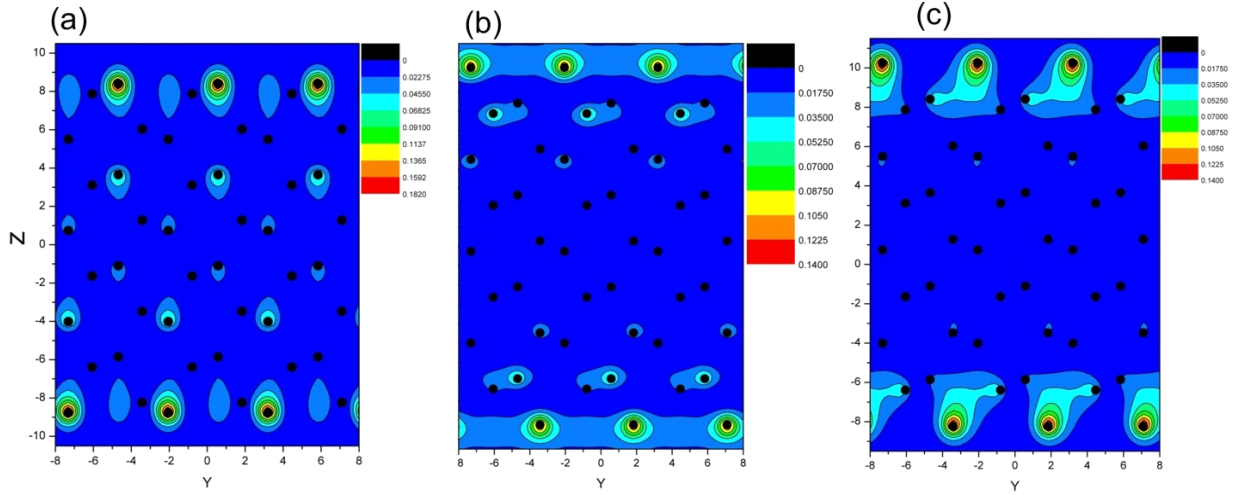


**Figure 4.** The charge density of the lower (out of 2) surface state at different high-symmetry points in the surface BZ and different types of terminations, for 4-unit-cell-thick films in the  $x=0$  plane. (a) at the  $\bar{Y}$  point for the *type a* termination. (b and c) at the  $\bar{\Gamma}$  and  $\bar{S}$  points, respectively, for the *type b* termination. Full black circles indicate the atomic positions. The surface atoms correspond to the top and bottom layers along the  $z$  direction. Note that the  $x=0$  plane coincides with that shown in Figs. 2 a,b.

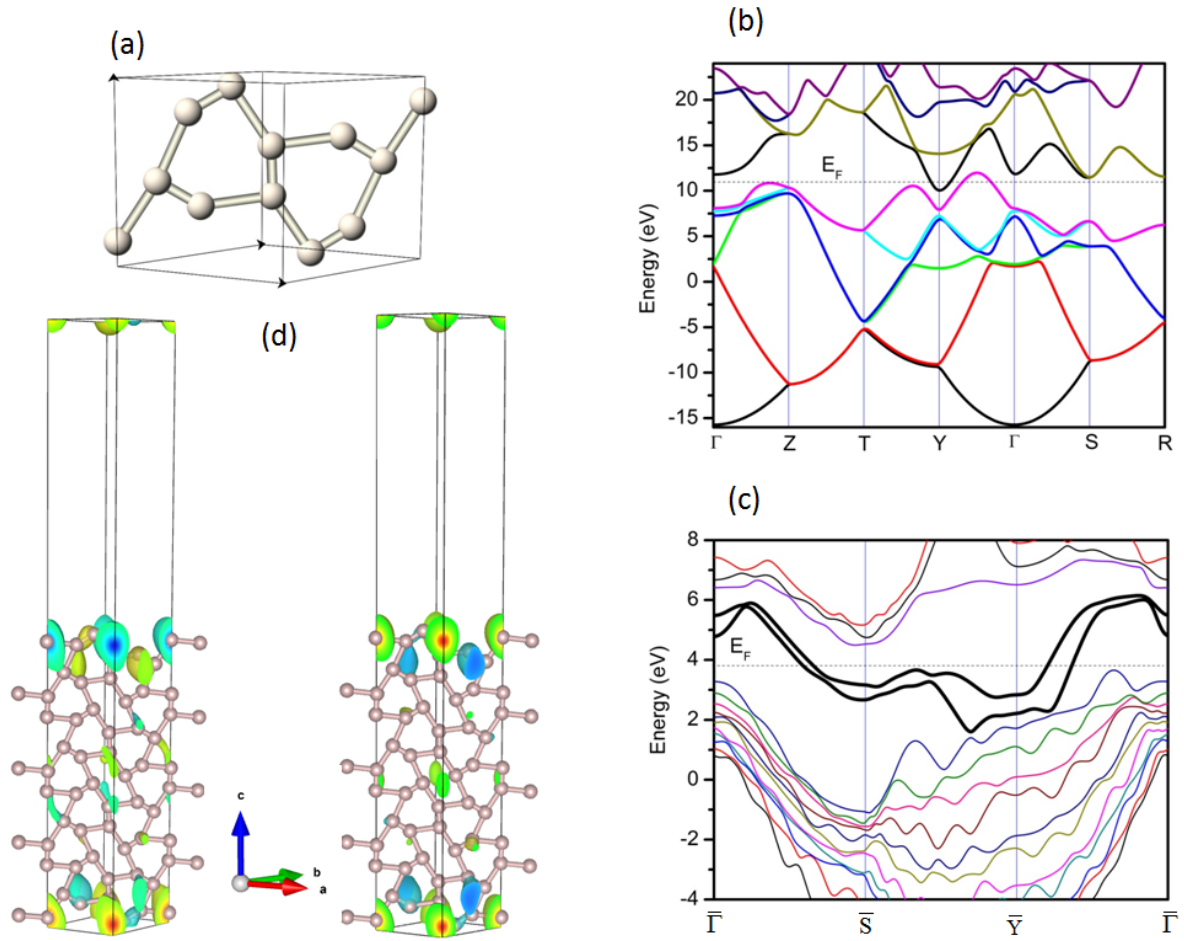


**Figure 5.** Crystal and band structures of the  $Cmca-12$  phase. (a) Primitive unit cell. (b) Bulk band structure at 300 GPa. (c) Band structure of a 4-unit-cell thick (001) film corresponding to the same pressure. The surface bands are indicated by thick black curves crossing the Fermi level. Their energies become equal to each other when the film thickness tends to infinity. (d) Isosurfaces ( $\pm 1.75$ ) of two Bloch functions at  $\bar{S}$  point: symmetric (right) and antisymmetric (left) with respect to the inversion center. The functions are shown in the used supercell consisting of atomic layers and vacuum gaps.